

SIMULATION OF THE ELECTROSTATIC DEFLECTOR OF DC140 CYCLOTRON

A. Zabanov[†], K. Gikal, G. Gulbekyan, I. Kalagin, N. Kazarinov, V. Lisov, S. Mitrofanov, V. Semin, JINR, 141980, Dubna, Russia

Abstract

The main activities of Flerov Laboratory of Nuclear Reactions, following its name - are related to fundamental science, but in parallel a lot of efforts are paid for practical applications. Currently, work is underway to create an irradiation facility based on the DC140 cyclotron for applied research at FLNR. The beam transport system will have three experimental beam lines for testing of electronic components (avionics and space electronics) for radiation hardness, for ion-implantation nanotechnology and for radiation materials science. The DC140 cyclotron is intended to accelerate heavy ions with mass-to-charge ratio A/Z within interval from 5 to 8.25 up to two fixed energies 2.124 and 4.8 MeV per unit mass. The intensity of the accelerated ions will be about 1 μA for light ions ($A < 86$) and about 0.1 μA for heavier ions ($A > 132$). The extraction system based on four main elements - electrostatic deflector (ESD), focusing magnetic channel, Permanent Magnet Quadrupole lens and steering magnet. The results of numerical simulation of the ESD of DC140 cyclotron are presented in this this paper.

INTRODUCTION

Flerov Laboratory of Nuclear Reaction of Joint Institute for Nuclear Research carries out the works under the creating of Irradiation Facility based on the DC140 cyclotron [1]. The DC140 will be a reconstruction of the DC72 cyclotron [2, 3].

The ion beam extraction process from the DC140 cyclotron is implemented using the ESD. The azimuthal extension of the ESD is 40° ($70^\circ - 110^\circ$). Due to the low power of the accelerated ion beams, it was decided that the potential electrode will not have an active cooling system.

The main criteria in the design of the ESD are the absence of electrical breakdowns between the electrodes and the minimum possible particle loss on the surface of the ESD.

This report presents the simulation and comparative analysis of various modifications of the ESD: with a constant gap and variable gap.

THE DETERMINATION OF CURVATURE RADIUS OF THE SEPTUM

The first step of the designing the ESD is determination of curvature radius of the septum. The extraction orbits of ion beams $^{40}\text{Ar}^{8+}$, $^{209}\text{Bi}^{38+}$ ($W = 4.8 \text{ MeV/u}$), $^{197}\text{Au}^{26+}$, $^{132}\text{Xe}^{16+}$ ($W = 2.124 \text{ MeV/u}$) were used to determine of curvature radius of the septum. The listed ion beams correspond to the corners of the working diagram of DC140 cyclotron (see Fig. 1).

[†] zabanov@jinr.ru

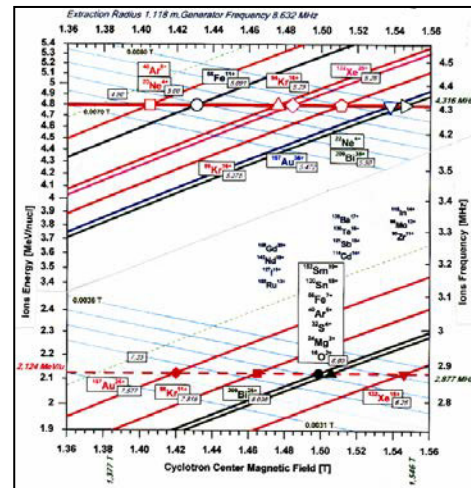


Figure 1: Working diagram of DC140 cyclotron.

The extraction orbit of ion beam in ESD can be represented as circular arc with center coordinates $(x_s; y_s)$. The optimization task is to find the curvature radius of the septum R_s and coordinates of the center $(x_s; y_s)$, which ensure the minimum value of the functional (Eq. 1).

$$\frac{1}{n} \sum_{i=1}^n (R_s - R_i)^2 \longrightarrow 0 \quad (1)$$

where $R_i = \sqrt{(r_i \cdot \cos(\varphi_i) - x_s)^2 + (r_i \cdot \sin(\varphi_i) - y_s)^2}$ is distance from the center coordinates $(x_s; y_s)$ to the i point of the extraction orbit of the ion beam, (r_i, φ_i) are the coordinates of point i of the extraction orbit of the ion beam in cylindrical coordinate system with origin in the cyclotron center.

The optimization results are presented in Table 1.

Table 1: the Optimization Results of the Determination of Curvature Radius of the Septum

Ion	W, MeV/u	x_s , cm	y_s , cm	R_s , cm
$^{40}\text{Ar}^{8+}$	4.8	20.87	-200.26	309.28
$^{209}\text{Bi}^{38+}$	4.8	19.01	-176.31	285.68
$^{197}\text{Au}^{26+}$	2.124	20.6	-198.67	307.68
$^{132}\text{Xe}^{16+}$	2.124	19.16	-177.33	286.71

The optimal values of curvature radii of the septum for the ion beams are very different from each other. It is necessary to find the value of curvature radius, which ensures the minimum beam losses. The curvature radius of the septum was chosen $R_s = 301.9 \text{ cm}$. This value was chosen from geometric and design considerations.

OPTIMIZATION OF CURVATURE RADIUS OF THE POTENTIAL ELECTRODE

Two modifications of ESD with a variable gap were considered in the work: with a linearly increasing gap and a linearly decreasing electrostatic field. The ratio of the inlet gap to the outlet gap of the ESD g_1/g_n is 6/9 (mm/mm). Let us consider in detail the modification of the ESD with a linearly decreasing field and a gap ratio of 6/9.

For convenience the following consideration will be performed in the local coordinate system $x'y'$. The center of the origin of coordinates of the local system coincides with the center of curvature of the septum. The ordinate axis y' passes through the centre of the septum. The azimuthal extension of the ESD $\Delta\varphi'$ in the local system is 14.73° ($[90^\circ - \Delta\varphi'/2; 90^\circ - \Delta\varphi'/2]$).

The field potential $F(r', \varphi')$ which provides a linearly decreasing field, is described by (Eq 2).

$$F(r', \varphi') = \frac{U}{\ln\left(\frac{R'_1}{R_s}\right)} \cdot \ln\left(\frac{r'}{R_s}\right) \quad (2)$$

where U is potential electrode voltage, R'_1 is distance from the center of coordinates to the inner surface of the potential electrode.

The distance R'_1 can be represented by a function of φ' (Eq. 3).

$$R'_1(\varphi') = R_s + g(\varphi') \quad (3)$$

The size of the gap $g(\varphi')$ is determined by the (Eq. 4):

$$g(\varphi') = R_s \cdot \exp\left(\frac{1}{C_1 + C_2 \cdot (\varphi' - \varphi'_n)}\right) \quad (4)$$

where C_1 and C_2 is entered coefficients, $C_1 = \ln\left(\frac{g_n}{R_s} + 1\right)$,

$$C_2 = \left[\frac{1}{\ln\left(\frac{g_1}{R_s} + 1\right)} - \frac{1}{\ln\left(\frac{g_n}{R_s} + 1\right)} \right] \cdot \frac{1}{\Delta\varphi'}$$

The optimization task is to find potential electrode radius of curvature R_{pot} and coordinates of the center (x'_{pot}, y'_{pot}), which ensure the minimum value of the functional (Eq. 5).

$$\frac{1}{n} \sum_{i=1}^n (R_{pot} - R'_{ii})^2 \longrightarrow 0 \quad (5)$$

The optimization results are presented in Table 2.

Table 2: the Results of Optimization of Curvature Radius of the Potential Electrode

g_1 [mm]	g_n [mm]	x'_{pot} [mm]	y'_{pot} [mm]	R_{pot} [cm]
6	9	11.64	-36.54	306.28

In Fig. 2 shows the graphs of the deviations δ of the resulting gap in azimuth from the gap for a linearly varying field.

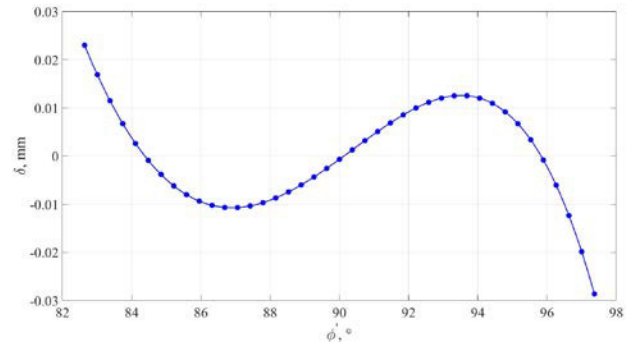


Figure 2: The deviations of the resulting gap in azimuth from the gap for a linearly varying field.

THE ELECTROSTATIC FIELD OF THE ESD WITH VARIABLE GAP

The electric field strength $E_{r'}$ and $E_{\varphi'}$ between the electrodes of the ESD is described by the following system of equations (6)

$$\begin{cases} E_{r'} = -U \cdot (C_1 + C_2 \cdot (\varphi' - \varphi'_n)) \cdot \frac{1}{r'} \\ E_{\varphi'} = -\frac{U \cdot C_2 \cdot \ln\left(\frac{r'}{R_s}\right)}{r'} \end{cases} \quad (6)$$

The 2D-model of the ESD was calculated using the FEMM 4.2. In Fig. 3 show graphs of the amplitude value of the electric field strength along the central trajectory of the ESD.

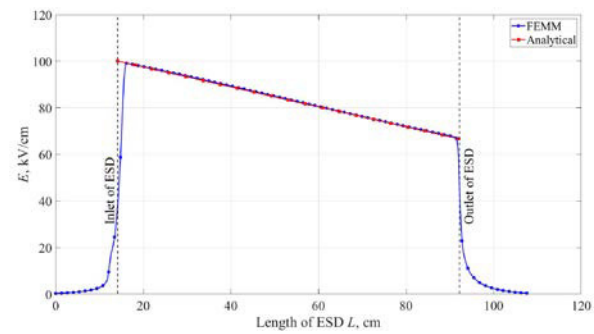


Figure 3: The amplitude value of the electric field strength along the central trajectory of the ESD.

THE COMPARISON OF VARIOUS MODIFICATIONS OF THE ESD

This section provides a comparative analysis of three modifications of the ESD: with constant gap $g = 9$ mm, with a linearly increasing gap ($g_1/g_n = 6/9$) and with a linearly decreasing electrostatic field ($g_1/g_n = 6/9$).

All of above modifications of the ESD deflect the ion beam at a given angle, i.e. integral of the electric field strength along the central trajectory of the ESD is the same for three modifications.

The beam losses is a key comparison criterion. The total beam losses η on the septum surface is the sum of three components:

1. losses at the inlet end face of septum η_{end} (Eq. 7)

$$\eta_{\text{end}} = \frac{d_s}{\Delta} \cdot 100\% \quad (7)$$

where d_s is septum thickness at its entry, $d_s = 0.5$ mm, Δ is casting of ion beam.

2. losses on the inner surface of the septum η_{in} (Eq. 8)

$$\eta_{\text{in}} = \frac{\min(\Delta R_s)^2}{4 \cdot \theta_{\text{max}} \cdot \Delta \cdot (L_s - L_{\text{loss}})} 100\% \quad (8)$$

where $\min(\Delta R_s)$ is minimum distance from the septum to the envelope of the extraction orbit, θ_{max} is the angle ion beam makes in the horizontal plane with respect to the assumed central trajectory, L_s is septum length, L_{loss} is distance from the entry ESD to the point at which beam losses begin.

3. losses on the outer surface of the septum η_{out} (Eq. 9)

$$\eta_{s2} = \frac{\min(\Delta R)^2}{4 \cdot l_{\text{min}} \cdot \theta_{\text{max}} \cdot \Delta} 100\% \quad (9)$$

where $\min(\Delta R)$ is the minimum distance from the septum to the envelope of the last acceleration orbit, l_{min} is distance from the entry ESD to the point at which the $\min(\Delta R)$.

The ESD is located according to the following rules:

1. there should be no beam losses at the potential electrode;
2. the centre of curvature of the septum ensures the minimum value of beam losses on the septum.

The orbits and envelopes calculated for ESD with a constant gap were used in calculating the particle losses at the septum. It was assumed that changes in the envelopes for the extraction orbit of ion beams are insignificant.

Figure 4 shows the estimated location of the ESD with a linearly decreasing electrostatic field for ion beam $^{209}\text{Bi}^{38+}$.

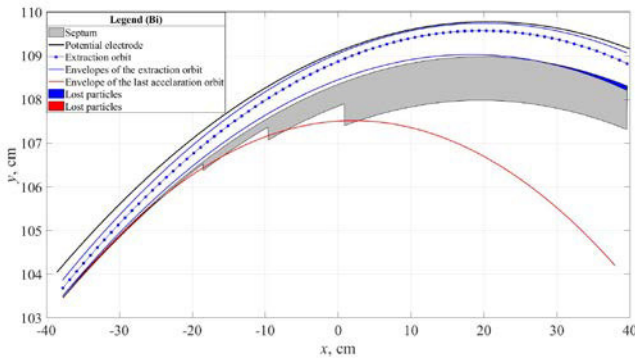


Figure 4: The estimated location of the ESD with a linearly decreasing electrostatic field for ion beam $^{209}\text{Bi}^{38+}$.

Table 3 shows a comparison of the various modifications of the ESD for ion beam $^{209}\text{Bi}^{38+}$ ($g_1/g_n = 6/9$).

High precision manufacturing of the potential electrode and its installation relative to the septum are important conditions for ensuring the desired change in the variable gap along the length of the ESD.

The ESD with constant gap between electrodes provides the lowest beam losses at the septum compared to the other modifications.

A big value of the beam losses of ion beam $^{209}\text{Bi}^{38+}$ is difference between the selected septum radius of curvature $R_s = 301.9$ cm and obtained as result of optimization for the extraction orbit ($R_{\text{Bi}} = 285.68$ cm).

Table 3: the Comparison of the Various Modifications of the ESD for Ion Beam $^{209}\text{Bi}^{38+}$

Parameter	Constant gap	Linearly gap	Linearly field
U [kV]	74	61.67	60.02
E_{max} [kV/cm]	82.22	101.44	99.11
$U \times E_{\text{max}}$ [kV ² /cm]	6084.3	6255.8	5948.6
η_{end} [%]	13.93	13.93	13.93
η_{in} [%]	0	9.04	15.75
η_{out} [%]	7.32	6.13	5.28
η [%]	21.25	29.1	34.96

P.S. beam losses are indicated for the ion $^{209}\text{Bi}^{38+}$, since they are of the greatest importance in total beam losses.

SUMMARY

The ESD modification with a constant gap was selected based on the minimum values of beam losses at the septum.

REFERENCES

- [1] S.V. Mitrofanov *et al.*, “FLNR JINR Accelerator Complex for Applied Physics Researches: State-of-Art and Future”, in *Proc. of 22nd Conf. on Cycl. and their Appl. 2019*, Cape Town, South Africa, Sep. 2019, pp. 358-360. doi : 10. 18429/ JACoW CYCLOTRONS2019- FRB02.
- [2] B. N. Gikal, “Dubna Cyclotrons – Status and Plans”, in *Proc. 17th Int. Conf. on Cyclotrons and Their Applications (Cyclotrons'04)*, Tokyo, Japan, Oct. 2004, paper 20A1, pp. 100-104.
- [3] G. Gulbekyan, I. Ivanenko, J. Franko, and J. Keniz, “DC-72 Cyclotron Magnetic Field Formation”, In *Proc. of 19th Russian Part. Acc. Conf (RuPAC'04)*, Dubna, Russia, Oct. 2004, paper WENO12, pp. 147-49.